www.czasopisma.pan.pl PAN www.journals.pan.pl

ARCHIVES of FOUNDRY ENGINEERING

ISSN (2299-2944)
Volume 2020
Issue 3/2020

15 – 20

10.24425/afe.2020.133323

3/3

Published quarterly as the organ of the Foundry Commission of the Polish Academy of Sciences

Compacted Graphite Iron with the Addition of Tin

G. Gumienny [a,] *, B. Kurowska [a], P. Fabian [b]

[a] Department of Materials Engineering and Production Systems, Lodz University of Technology, Stefanowskiego 1/15 Street, 90-924 Łódź, Poland

[b] Department of Technological Engineering, University of Žilina, Univerzitná 8215/1, 010 26 Žilina

* Corresponding author. E-mail address: grzegorz.gumienny@p.lodz.pl

Received 04.12.2019; accepted in revised form 20.03.2020

Abstract

The paper presents the effect of tin on the crystallization process, microstructure and hardness of cast iron with compacted (vermicular) graphite. The compacted graphite was obtained with the use of magnesium treatment process (Inmold technology). The lack of significant effect of tin on the temperature of the eutectic transformation has been demonstrated. On the other hand, a significant decrease in the eutectoid transformation temperature with increasing tin concentration has been shown. It was demonstrated that tin narrows the temperature range of the austenite transformation. The effect of tin on the microstructure of cast iron with compacted graphite considering casting wall thickness has been investigated and described. The carbide-forming effect of tin in thin-walled (3 mm) castings has been demonstrated. The nomograms describing the microstructure of compacted graphite iron versus tin concentration have been developed. The effect of tin on the hardness of cast iron was given.

Keywords: Theory of crystallization, Compacted graphite iron, Tin, Cooling and derivative curves

1. Introduction

Although the initial attention of the foundry industry focused on ductile iron, efforts began in the early 1960's to develop Compacted Graphite Iron (CGI) production techniques and product applications. Since then, many CGI applications have been successfully established in series production. This form of cast iron is being used for the manufacture of brake disks, exhaust manifolds, cylinder heads, as well as diesel engine blocks. CGI diesel engine blocks are, inter alia, produced for: Mercedes, MAN, DAF, Volvo, Audi, Ford or Hyundai [1].

However, the production of cast iron with compacted graphite makes many problems. One of them is the need to maintain a high technological regime, including maintaining a magnesium concentration in a very narrow range. Schematically this is shown in Figure 1.

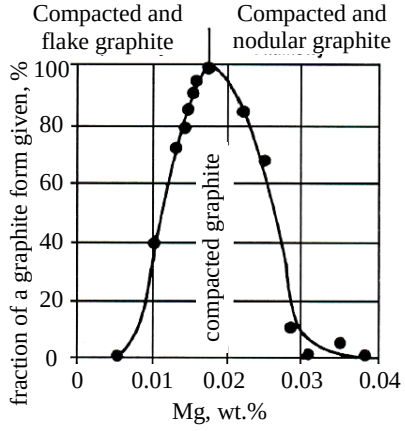

Fig. 1. The effect of Mg on the graphite proportion [2]

In accordance with PN-EN 16079: 2012 compacted graphite iron shall contain 80% minimum type III graphite. The rest of precipitations may be characterized by the type IV, V and VI in accordance with PN-EN ISO 945-1:2008.

The standard specifies five grades CGI with a tensile strength of 300 to 500 MPa at an elongation from 2.0 to 0.5%, respectively. Cast iron matrix changes from the predominantly ferritic (EN-GJV-300) to the pearlitic (EN-GJV-500).

The change of the matrix microstructure can be caused by modification of the chemical composition. Data concerning the influence of alloying additives on the CGI matrix can be found in [3-5]. Alloy additions are usually designed to increase the mechanical properties of cast iron by changing the metal matrix. Then pearlite-forming elements are used. Copper is a well-known and often used element with this effect [6-8]. As an alloying additive it is even used in an austenitic cast iron [9]. Tin is an element that intensively promotes the formation of pearlite. It is problematic when used for cast iron with nodular or compacted graphite because it leads to the degeneration of the graphite shape. This is especially the case for smelting cast iron with a large amount of impurities. There is quite a lot of literature data concerning the effect of tin in cast iron [10-13], however, these data are even from several decades ago. There are significant deficiencies in the literature regarding the effect of tin on the crystallization process, microstructure and properties of compacted graphite iron. Some data can be found in [14, 15]. Accordingly, the aim of this study is to investigate the effect of tin on the crystallisation, microstructure and hardness of cast iron with compacted graphite. The castings with 3-24 mm wall thickness cooled inside the sand mould were tested.

2. Methodology

A metallic charge was melted in an electric medium-frequency induction crucible furnace of 30 kg capacity. It consisted of a special pig iron with reduced sulfur content, ferro-silicon, ferro-manganese and technically pure tin.

Compacted graphite was obtained using Inmold technology. Schematic layout of elements in the mould is presented in Figure 2.

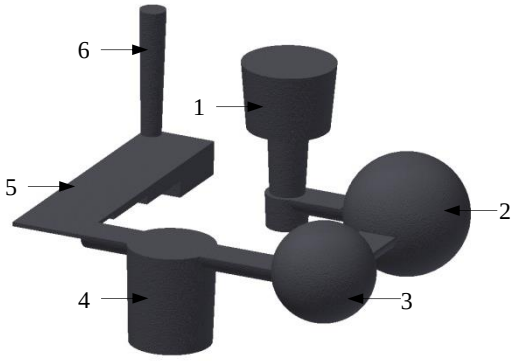

Fig. 2. Schematic layout of elements in the mould: 1 – downsprue, 2 - reaction chamber, 3 – mixing chamber, 4 – control chamber, 5 – stepped test casting, 6 – flow off

The pouring temperature was approx. 1480°C. In the reaction chamber (2) the magnesium master alloy was placed. Its chemical composition is shown in Table 1. The reaction chamber has the shape of a sphere, which is the most advantageous due to the graphite yield [16]. The liquid alloy through the mixing chamber (3) flooded the control chamber (4). In its thermal center, the PtRh10-Pt thermocouple (type S) was located to registration the cooling and crystallization process. As a next step, the liquid iron filled the mould cavity (5) and flow off (6). The tested casting was characterized by the wall thickness 3, 6, 12 and 24 mm.

Table 1.
The chemical composition of the master alloy

Chemical composition, wt.%					
Si	Mg	Ca	La	Al	Fe
44÷48	5÷6	0.4÷0.6	0.25÷0.40	0.8÷1.2	rest

Magnesium and lanthanum are the nodulizers in the master alloy. There are also calcium and aluminum as inoculants, while silicon is a graphite-forming element.

The chemical composition of the CGI tested is presented in Table 2.

Table 2.
The chemical composition of the CGI tested

No.	Chemical composition, wt.%						
	C	Si	Mn	P	S	Sn	Mg
1.	3.42	2.53	0.27	0.05	0.008	-	0.017
2.	3.47	2.38	0.32	0.07	0.010	0.031	0.017
3.	3.42	2.53	0.33	0.07	0.013	0.061	0.018
4.	3.49	2.59	0.33	0.07	0.014	0.081	0.018
5.	3.47	2.50	0.30	0.06	0.010	0.121	0.019

The concentration of carbon, silicon and manganese was kept at a typical level. The phosphorus concentration did not exceed 0.07%, while sulfur – 0.014%. The tin content was changed to a maximum of 0.12% in steps of 0.3-0.4%. The concentration of magnesium in cast iron ranged from 0.017 to 0.019%. The change in Mg concentration was dictated by the negative effect of tin on the graphite shape. Specimens for metallographic studies were cut from the central part of the stepped casting. After grinding and polishing they were etched with a 4% HNO_3 solution in C_2H_5OH. The Nikon Eclipse MA200 optical microscope and magnification ×500 were used to the metallographic examinations. The fraction of phases in the microstructure was tested using the NIS-Elements-BR program.

The hardness of the cast iron was examined on specimens cut-off from the casting with wall thickness of 24 mm with the HPO-2400 hardness tester using a test load of 1840 N, a ball of diameter 2.5 mm and the dwell time 15 s.

3. Results

In Figure 3 (a, b) cooling curves and their derivative of non-alloyed CGI in the crystallization area (a) and solid state transformation (b) are presented.

a)

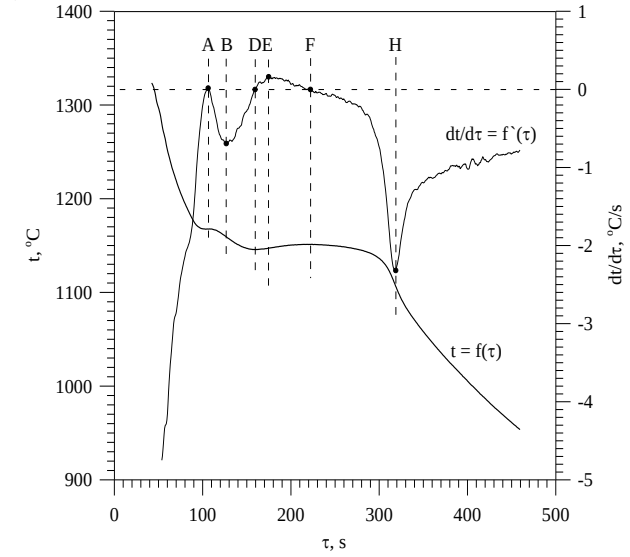

b)

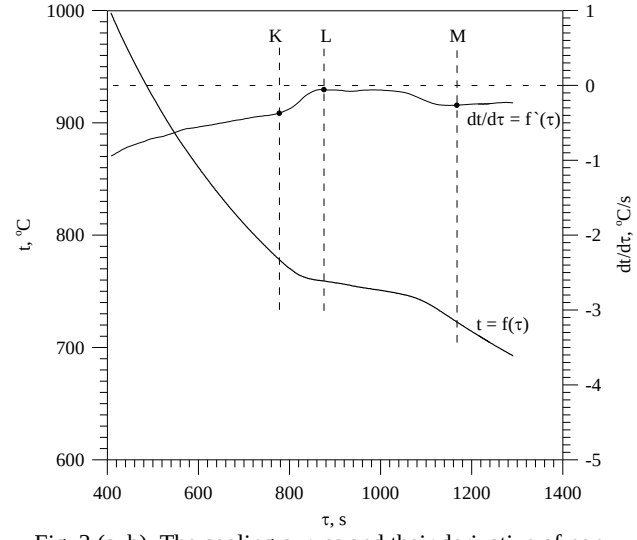

Fig. 3 (a, b). The cooling curves and their derivative of non-alloyed CGI: (a) crystallization area, (b) solid state transformation area

There are three thermal effects described by characteristic points on derivative curves (two in Fig. 3a) and one in Fig. 3b). AB thermal effect comes from the transformation of a liquid into the primary austenite. The transformation of the liquid into the eutectic mixture of the compacted graphite and austenite causes DEFH thermal effect. Crystallization of the non-alloyed cast iron finishes at 1107°C (point H). The austenite transformation takes place at a temperature of 775-745°C (KLM thermal effect – Fig. 3b).

The addition of tin in CGI did not change the number of thermal effects. The end of cast iron crystallization took place at a slightly lower temperature, while a significant difference in the range of solid state transformation is visible. The increase in tin concentration resulted in a significant decrease in the austenite transformation temperature.

In Table 3 the temperature of the phase transformations in CGI tested is presented.

Table 3.
The temperature of the phase transformations in CGI tested

Sn, wt.%	t, °C					
	tA	tD	tF	tH	tK	tM
0.00	1168	1146	1151	1107	775	745
0.03	1153	1150	1155	1106	758	733
0.06	1203	1152	1157	1111	750	727
0.08	1208	1149	1151	1107	748	728
0.12	1168	1145	1149	1102	739	724

From the data presented in Tab. 3 results that tin did not significantly change the maximum temperature of the eutectic transformation (point F) as well as the temperature at the end of austenite + graphite eutectic crystallization (point H). For cast iron containing 0.12% Sn, the austenite transformation starts at a temperature 36°C lower compared to cast iron without the addition of tin, and finishes at a temperature lower by 21°C. It follows that a significant (approximately double) reduce the range of the transformation in the solid state temperature. The effect of tin on the eutectic transformation temperature is presented graphically in Figure 4, while on the transformation in solid state in Figure 5.

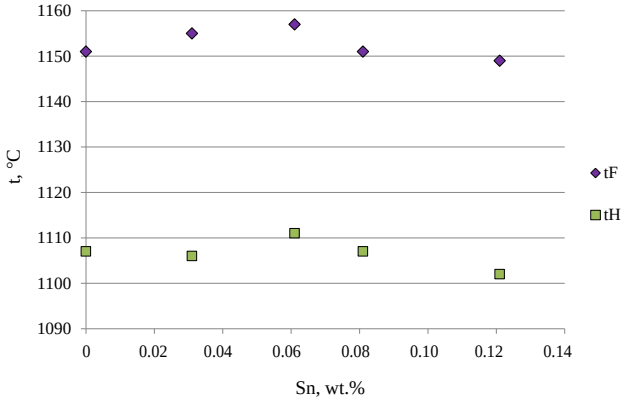

Fig. 4. The temperature of the eutectic transformation vs tin concentration in CGI tested

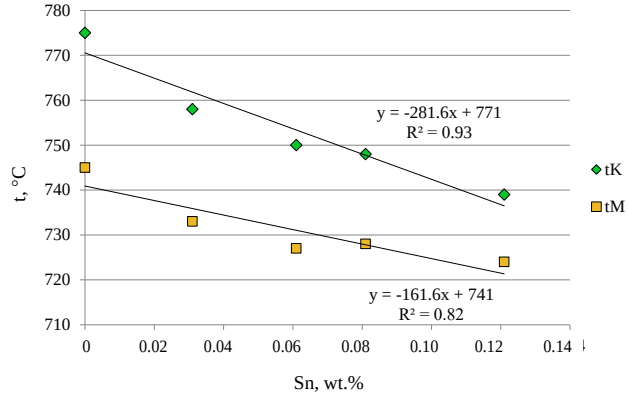

Fig. 5. The temperature of the eutectoid transformation vs tin concentration in CGI tested

Fig. 4 shows that the maximum temperature of the eutectic mixture crystallisation (tF) did not change significantly; a temperature by several degrees Celsius higher in cast iron with the addition of 0.03 and 0.06% Sn has been recorded. However, a slight decrease in the temperature at the end of the graphite eutectic crystallisation (tH) can be noticed.

Fig. 5 shows that tin in cast iron with compacted graphite decreases the temperature of the austenite transformation start (tK) by about 28°C per 0.1% while the temperature of the austenite transformation finish (tM) by about 28°C per 0.1%

Figure 6 shows the microstructure of the non-alloyed CGI in castings with a wall thickness of 3 mm (a) and 24 mm (b).

a)

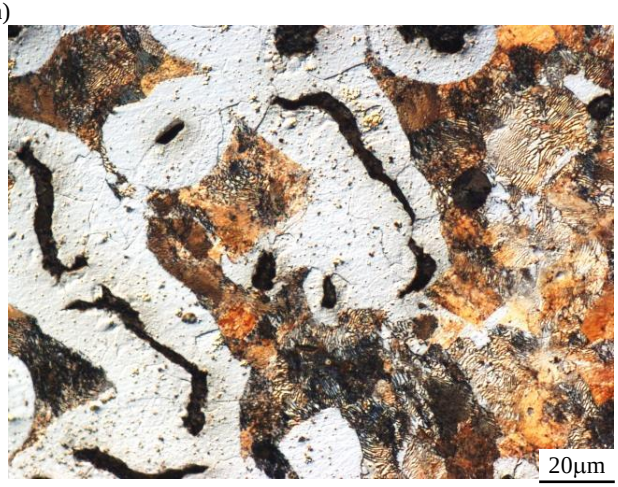

b)

Fig. 6. The microstructure of non-alloyed compacted graphite iron in castings with wall thickness: a) 3 mm; b) 24 mm

From Fig. 6 results, the microstructure in a 3 mm wall thickness castings consists of compacted graphite (~4%), pearlite (~68%) and ferrite (~28%). In thick-walled castings, the pearlite fraction was ~24%, ferrite ~72%, while graphite ~ 4%.

In Figure 7 the microstructure of the CGI containing about 0.03% Sn in castings with a wall thickness of 3 mm (a) and 24 mm (b) is presented.

a)

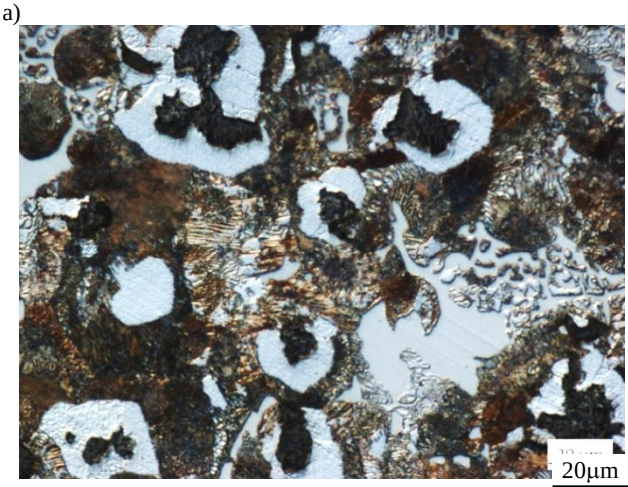

b)

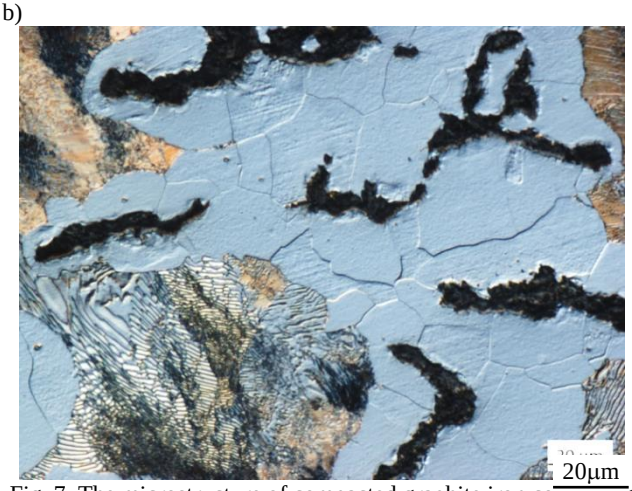

Fig. 7. The microstructure of compacted graphite iron containing approx. 0.03% Sn in castings with wall thickness: a) 3 mm; b) 24 mm

The small addition of tin causes the precipitation of carbides at the boundaries of eutectic grains in thin-walled castings. The volume fraction of ferrite clearly decreased (from 26% to 12%). Fe_3C carbides were not observed in castings with a wall thickness of 6-24 mm. The maximum fraction of ferrite was 44% (in castings with a wall thickness of 24 mm - Fig. 7b) – it was almost twice smaller compared to unalloyed cast iron.

The microstructure of CGI containing about 0.12% Sn in castings with a wall thickness of 3 mm and 24 mm is shown in Figure 8.

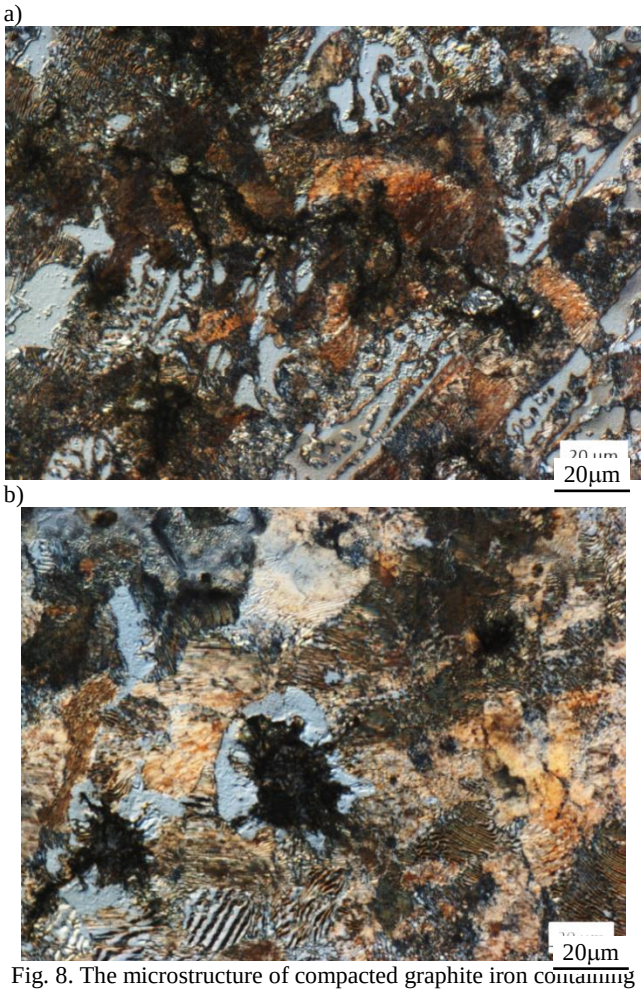

Fig. 8. The microstructure of compacted graphite iron containing approx. 0.12% Sn in castings with wall thickness: a) 3 mm; b) 24 mm

Despite the addition of 0.12% Sn, there was slight precipitations of ferrite near to the graphite in both thin-walled and thick-walled castings. This is most likely due to the tendency of compacted graphite iron to form ferrite. In thin-walled castings (3 mm), the fraction of carbides increased to about 10%.

In Figure 9 the microstructure components vs. tin concentration in castings with wall thickness 3-24 mm is presented. It shows that in thin-walled castings (Fig. 9a) the addition of tin causes the precipitation of cementite. In castings with a wall thickness of 6 mm (Fig. 9b), there was no cementite precipitations. The amount of pearlite and ferrite in the abovementioned castings were similar in the tested tin concentration range; a similar fact was observed in castings with a wall thickness of 12 and 24 mm (Fig. 9c and 9d). No "pure" pearlitic cast iron matrix was obtained in the cast iron tested.

The hardness of CGI vs. tin concentration is presented in Figure 10. It follows that tin increases the CGI hardness by about 100 HB per 0.1% concentration (i.e. from about 180 HB for cast iron without the addition of Sn to about 300 HB at a concentration of about 0.12% Sn). It is of course due to the fact that it is a pearlite-forming element.

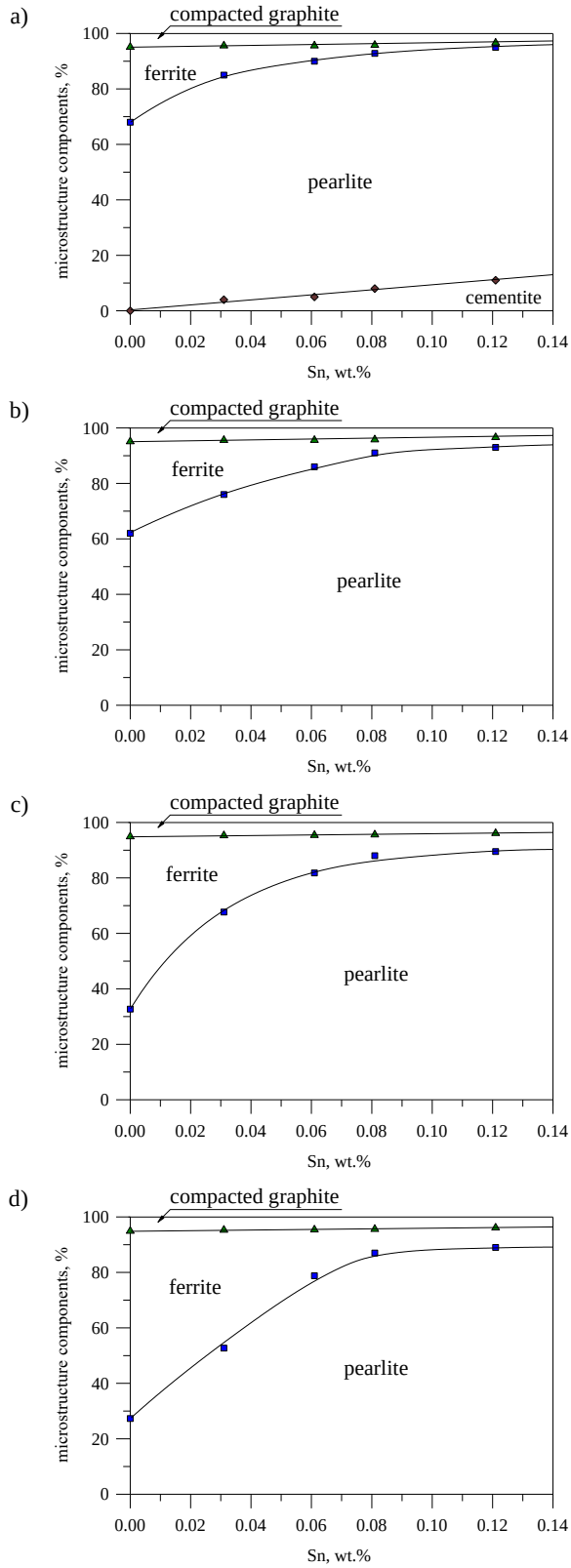

Fig. 9. Microstructure components vs. tin concentration in castings with wall thickness: a) 3 mm, b) 6 mm, c) 12 mm, d) 24 mm

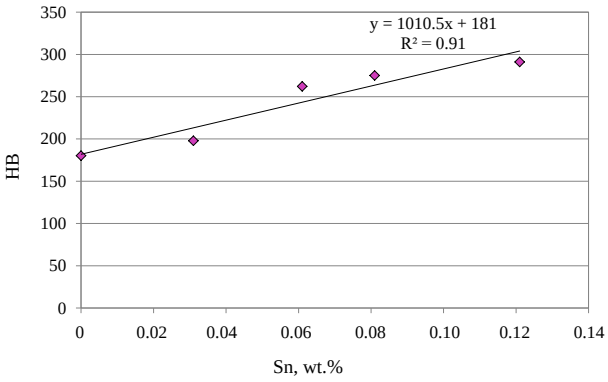

Fig. 10. CGI hardness vs tin concentration

4. Conclusions

The results of the research predestine to the following conclusions:

- there was no significant effect of tin on the eutectic transformation temperature in cast iron with compacted graphite,
- tin decreases the temperature of the austenite transformation start by about 28°C per 0.1% concentration, while the end decreases by about 16°C per 0.1% concentration. Simultaneously, it narrows the temperature range of the austenite transformation,
- the addition of 0.12% Sn does not result in a completely pearlitic matrix of compacted graphite iron, even in thin-walled castings,
- tin causes carbides crystallization in castings with a wall thickness of 3 mm at a concentration of 0.03%,
- tin increases the hardness of compacted graphite iron castings by about 100 HB units per 0.1% concentration.

References

[1] Folkson, R. (Ed.). (2014). *Alternative fuels and advanced vehicle technologies for improved environmental performance: towards zero carbon transportation*. Elsevier.

[2] Guzik, E. (2001). Some selected problems concerning the processes of cast iron improvement. *Monograph, 1M. Archives of Foundry*. (in Polish).

[3] Choong-Hwan, L. & Byeong-Choon, G. (2011). Development of compacted vermicular graphite cast iron for railway brake discs. *Metals and Materials International*. 17(2), 199-205. DOI: 10.1007/s12540-011-0403-x.

[4] Hosdez, J., Limodin, N., et al. (2019). Fatigue crack growth in compacted and spheroidal graphite cast irons. *International Journal of Fatigue*. 105319.

[5] Lopez-Covaleda, E.A., Ghodrat, S., Kestens, L., Sacre, C. H., & Pardoen, T. (2018). Proposal of characterization procedure of metal-graphite interface strength in compacted graphite iron. *Materials (Basel, Switzerland)*. 11(7), 1159. DOI:10.3390/ma11071159.

[6] Popov, P.I. & Sizov, I.G. (2006). Effect of alloying elements on the structure and properties of iron with vermicular graphite. *Metal Science and Heat Treatment*. 48(5-6), 272-275.

[7] König, M., & Wessén, M. (2009). The influence of copper on microstructure and mechanical properties of compacted graphite iron. *International Journal of Cast Metals Research*. 22(1-4), 164-167.

[8] Megahed, H., El-Kashif, E., Shash, A. Y., & Essam, M. A. (2019). Effect of holding time, thickness and heat treatment on microstructure and mechanical properties of compacted graphite cast iron. *Journal of Materials Research and Technology*. 8(1), 1188-1196.

[9] Medyński, D., & Janus, A. (2015). Effect of nickel equivalent on structure and corrosion resistance of nodular cast iron Ni-Mn-Cu. *Archives of Foundry Engineering*. 15(spec.1), 69-74.

[10] Ye, Z., Zhang, C., Wang, Y., Cheng, H. S., Tung, S., Wang, Q. J., & He, X. (2004). An experimental investigation of piston skirt scuffing: a piston scuffing apparatus, experiments, and scuffing mechanism analyses. *Wear*. 257(1-2), 8-31.

[11] Lacaze, J., & Sertucha, J. (2016). Effect of Cu, Mn and Sn on pearlite growth kinetics in as-cast ductile irons. International. *Journal of Cast Metals Research*. 29(1-2), 74-78.

[12] Guerin, L., & Gagné, M. (1987). Effect of manganese, copper and tin on the microstructure and properties of ductile iron castings. *Foundryman*, 80(7), 336-344.

[13] Kataoka, Y., Itoh, T., Higuchi, M. & Murai, K. (1987). Effects of Tin addition on spheroidal graphite cast iron. *The Journal of the Japan Foundrymen's Society*. 59(2), 74-78.

[14] Lyu, Y. (2019). Abrasive wear of compacted graphite cast iron with added Tin. *Metallography, Microstructure, and Analysis*. 8(1), 67-71.

[15] Lyu, Y., Sun, Y., Liu, S., & Zhao, J. (2015). Effect of tin on microstructure and mechanical properties of compacted graphite iron. *International Journal of Cast Metals Research*. 28(5), 263-268.

[16] Pietrowski, S. (2010). Influence of reaction chamber shape on cast-iron spheroidization process in-mold. *Archives of Foundry Engineering*. 10(1), 115-122.